Inorg. Chem. **2005**, *44*, 9534–9541

Tetranuclear Platinum Phosphido Complexes with Different Structures†

Juan Forniés,* Consuelo Fortuño, Reyes Gil, and Antonio Martín

Departamento de Química Inorgánica, Instituto de Ciencia de Materiales de Aragón, Universidad de Zaragoza, CSIC, E-50009 Zaragoza, Spain

Received July 26, 2005

The addition of $[NBu_4]Br$ or $[NBu_4][BH_4]$ to solutions of $[Pt_4(\mu\text{-}PPh_2)_4(C_6F_5)_4(CO)_2]$ (**3**) yields the complexes $[NBu_4]_2[Pt_4(\mu\text{-}PPh_2)_4(\mu\text{-}X)_2(C_6F_5)_4]$ (X = Br, **4**; H, **5**) in which the two CO groups have been replaced by two anionic, bridging X ligands. The total valence electron counts are 64 and 60, respectively; thus, complex **4** does not require Pt–Pt bonds, while two metal–metal bonds are present in **5**, as their NMR spectra confirm. Also, the NMR spectra indicate a nonsymmetrical "$Pt(\mu\text{-}PPh_2)_2Pt(\mu\text{-}PPh_2)(\mu\text{-}X)Pt(\mu\text{-}PPh_2)(\mu\text{-}X)Pt$" disposition for **4** and **5**. Treatment of **5** with HX (X = Cl, Br) yields the complexes $[NBu_4]_2[Pt_4(\mu\text{-}PPh_2)_4(\mu\text{-}H)_2(C_6F_5)_3X]$ (X = Cl, **6**; Br, **7**). These complexes react with $[Ag(OClO_3)PPh_3]$ with displacement of the halide and formation of $[NBu_4][Pt_4(\mu\text{-}PPh_2)_4(\mu\text{-}H)_2(C_6F_5)_3\text{-}PPh_3]$ (**8**). Complexes **6**–**8** maintain the same basic skeleton as **5**, with two Pt–Pt bonds. Complex **4** is, however, an isomer of the symmetric $[NBu_4]_2[\{(C_6F_5)_2Pt(\mu\text{-}PPh_2)_2Pt(\mu\text{-}Br)\}_2]$ (**9**), which has been prepared by a metathetical process from the well-known $[NBu_4]_2[\{(C_6F_5)_2Pt(\mu\text{-}PPh_2)_2Pt(\mu\text{-}Cl)\}_2]$ (**1**). The comparison of the X-ray structures of **4** and **9** confirms the different disposition of the bridging ligands, and their main structural differences seem to be related to the size of Br^- and its position in the skeleton.

Introduction

The known ability of the phosphido ligands to form polynuclear metal complexes in which the metal centers are supported by these bridging ligands has produced a very rich and interesting chemistry.[1−13] Although it was originally thought that the flexibility and stability of the M−P bonds allowed the polynuclear complexes to be maintained, several transformations[14−17] and peculiar coordination modes[18−25] of

* To whom correspondence should be addressed. E-mail: juan.fornies@unizar.es.

† Polynuclear Homo- or Heterometallic Palladium(II)−Platinum(II) Pentafluorophenyl Complexes Containing Bridging Diphenylphosphido Ligands. 18. Part 17: Ara, I.; Chaouche, N.; Forniés, J.; Fortuño, C.; Kribii, A.; Martín, A. *Eur. J. Inorg. Chem.* **2005**, 3894−3901.

(1) Alonso, E.; Forniés, J.; Fortuño, C.; Martín, A.; Rosair, G. M.; Welch, A. J. *Inorg. Chem.* **1997**, *36*, 4426−4431.
(2) Mizuta, T.; Onishi, M.; Nakazono, T.; Nakazawa, H.; Miyoshi, K. *Organometallics* **2002**, *21*, 717−726.
(3) Leoni, P.; Marchetti, F.; Pasquali, M.; Marchetti, L.; Albinati, A. *Organometallics* **2002**, *21*, 2167−2182.
(4) Bender, R.; Braunstein, P.; Dedieu, A.; Ellis, P. D.; Huggins, B.; Harvey, P. D.; Sappa, E.; Tiripicchio, A. *Inorg. Chem.* **1996**, *35*, 1223−1234.
(5) Chaouche, N.; Forniés, J.; Fortuño, C.; Kribii, A.; Martín, A.; Karipidis, P.; Tsipis, A. C.; Tsipis, C. A. *Organometallics* **2004**, *23*, 1797−1810.
(6) Archambault, C.; Bender, R.; Braunstein, P.; Dusausoy, Y. *J. Chem. Soc., Dalton Trans.* **2002**, 4084−4090.
(7) Leoni, P.; Pasquali, M.; Fadini, L.; Albinati, A.; Hofmann, P.; Metz, M. *J. Am. Chem. Soc.* **1997**, *119*, 8625−8629.
(8) Bender, R.; Braunstein, P.; Bouaoud, S. E.; Rouag, D.; Harvey, P. D.; Golhen, S.; Ouahab, L. *Inorg.* Chem. **2002**, *41*, 1739−1746.
(9) Itazaki, M.; Nishihara, Y.; Osakada, K. *Organometallics* **2004**, *23*, 1610−1621.
(10) Heyn, R. H.; Gorbitz, C. H. *Organometallics* **2002**, *21*, 2781−2784.
(11) Alonso, E.; Casas, J. M.; Cotton, F. A.; Feng, X. J.; Forniés, J.; Fortuño, C.; Tomás, M. *Inorg. Chem.* **1999**, *38*, 5034−5040.
(12) Falvello, L. R.; Forniés, J.; Fortuño, C.; Durán, F.; Martín, A. *Organometallics* **2002**, *21*, 2226−2234.
(13) Alonso, E.; Forniés, J.; Fortuño, C.; Martín, A.; Orpen, A. G. *Organometallics* **2003**, *22*, 5011−5019.
(14) Forniés, J.; Fortuño, C.; Ibáñez, S.; Martín, A.; Tsipis, A. C.; Tsipis, C. A. *Angew. Chem., Int. Ed.* **2005**, *44*, 2407−2410.
(15) Falvello, L. R.; Forniés, J.; Fortuño, C.; Martín, A.; Martínez-Sariñena, A. P. *Organometallics* **1997**, *16*, 5849−5856.
(16) Albinati, A.; Filippi, V.; Leoni, P.; Marchetti, L.; Pasquali, M.; Passarelli, V. *Chem. Commun.* **2005**, 2155−2157.
(17) Archambault, C.; Bender, R.; Braunstein, P.; De Cian, A.; Fischer, J. *Chem. Commun.* **1996**, 2729−2730.
(18) Alonso, E.; Forniés, J.; Fortuño, C.; Martín, A.; Orpen, A. G. *Organometallics* **2000**, *19*, 2690−2697.
(19) Alonso, E.; Forniés, J.; Fortuño, C.; Martín, A.; Orpen, A. G. *Organometallics* **2003**, *22*, 2723−2728.
(20) Bender, R.; Braunstein, P.; Dedieu, A.; Dusausoy, Y. *Angew. Chem., Int. Ed. Engl.* **1989**, *28*, 923−925.
(21) Wicht, D. K.; Kourkine, I. V.; Lew, B. M.; Nthenge, J. M.; Glueck, D. S. *J. Am. Chem. Soc.* **1997**, *119*, 5039−5040.
(22) Zhuravel, M. A.; Glueck, D. S.; Zakharov, L. N.; Rheingold, A. L. *Organometallics* **2002**, *21*, 3208−3214.
(23) Rabe, G. W.; Kheradman, S.; Liable-Sands, L. M.; Guzei, I. A.; Rheingold, A. L. *Angew. Chem., Int. Ed.* **1998**, *37*, 1404−1407.
(24) Frenzel, C.; Somoza, F. J.; Blaurock, S.; Hey-Hawkins, E. *J. Chem. Soc., Dalton Trans.* **2001**, 3115−3118.
(25) Englich, U.; Hassler, K.; Ruhlandt-Senge, K.; Unlig, F. *Inorg. Chem.* **1998**, *37*, 3532−3537.

10.1021/ic051248y CCC: $30.25
Published on Web 11/12/2005

Scheme 1

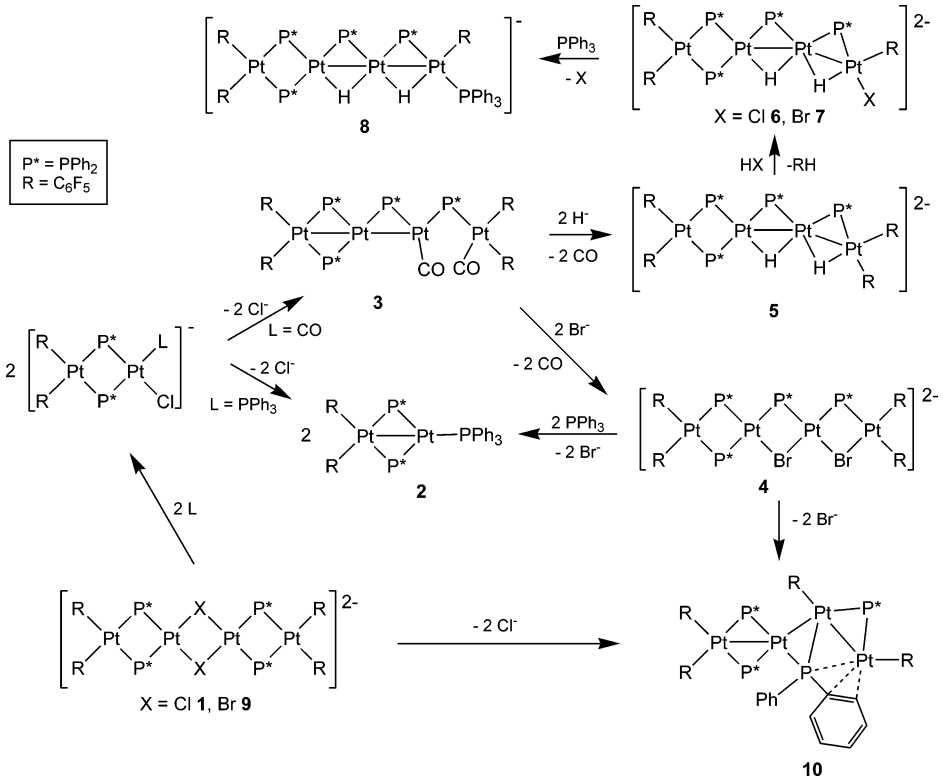

the phosphido ligands have been described, making this field more attractive.

Earlier we studied the reaction of the tetranuclear complex $[NBu_4]_2[\{(C_6F_5)_2Pt(\mu\text{-}PPh_2)_2Pt(\mu\text{-}Cl)\}_2]$ (**1**), with L (PPh_3, CO) in a 1:2 molar ratio, which results in the bridge cleavage of the $Pt(\mu\text{-}Cl)_2Pt$ moiety, producing the dinuclear anionic derivative $[(C_6F_5)_2Pt(\mu\text{-}PPh_2)_2PtClL]^-$. However, the elimination of the terminal chloride with $AgClO_4$ surprisingly results in very different complexes because when L = PPh_3, the dinuclear derivative $[(C_6F_5)_2Pt(\mu\text{-}PPh_2)_2PtPPh_3]$ (**2**), with a 30 valence electron count and hence a Pt−Pt bond, is obtained.[26] When L = CO, the tetranuclear cluster $[Pt_4(\mu\text{-}PPh_2)_4(C_6F_5)_4(CO)_2]$ (**3**; 60 valence electron count), with two Pt−Pt bonds and two terminal CO ligands, is obtained (Scheme 1).[15]

In this paper, we study the reaction of complex **3**, which contains two labile CO ligands with H^- and Br^-. These ligands displace CO and, although both can act as terminal or bridging ligands, hydride is exclusively a two-electron donor while bromide can potentially provide a higher number of electrons. This fact is clearly reflected in the nature of the resulting complexes, the reactivity of which is also studied.

Results and Discussion

The addition of $[NBu_4]Br$ or $[NBu_4][BH_4]$ to solutions of **3** (2:1 molar ratio) yields the dianionic complexes $[NBu_4]_2[Pt_4(\mu\text{-}PPh_2)_4(\mu\text{-}X)_2(C_6F_5)_4]$ (X = Br, **4**; H, **5**) in which the two CO groups have been replaced by two bridging X ligands (Scheme 1). The total valence electron counts are 64 and 60, respectively; thus, complex **4** does not require Pt−Pt bonds, while two metal−metal bonds have to be present in the tetranuclear **5**, as is depicted in Scheme 1. The three-center two-electron interaction (3c−2e) in a "PtHPt" unit may also be described as a protonated metal−metal bond.[27,28]

The most significant data in the IR spectra of these tetranuclear derivatives are the presence of an absorption to ca. 880 cm^{-1} due to the counterion $[NBu_4]^+$ along with the absence of absorptions due to the CO ligands. It is well-known that the $\nu(Pt-H_{terminal})$ stretching mode is usually observed in the range 1970−2250 cm^{-1}, while for the bridging hydride, such absorptions (ca. 1600 cm^{-1}) are usually weak and often difficult to assign.[9,29−33] In complex **5**, we have not been able to locate any absorption either in the terminal region or in the bridging region.

The ^1H NMR spectra of **4** and **5** show signals due to the hydrogen atoms of the phenyl groups along with those due to the counterion $[NBu_4]^+$. Their relative intensities are in agreement with the proposed dianionic nature of the complexes. In **5**, two signals due to hydride ligands are observed.

(26) Falvello, L. R.; Forniés, J.; Fortuño, C.; Martínez, F. *Inorg. Chem.* **1994**, *33*, 6242−6246.

(27) Zhuravel, M. A.; Moncarz, J. R.; Glueck, D. S.; Lam, K.-C.; Rheingold, A. L. *Organometallics* **2000**, *19*, 3447−3454.

(28) van Leeuwen, P. W. N. M.; Roobeek, C. F.; Frijns, J. H. G.; Orpen, A. G. *Organometallics* **1990**, *9*, 1211−1222.

(29) Leoni, P.; Pasquali, M.; Fortunelli, A.; Germano, G.; Albinati, A. *J. Am. Chem. Soc.* **1998**, *120*, 9564−9573.

(30) Leoni, P.; Manetti, S.; Pasquali, M. *Inorg. Chem.* **1995**, *34*, 749−752.

(31) Alonso, E.; Forniés, J.; Fortuño, C.; Martín, A.; Orpen, A. G. *Organometallics* **2001**, *20*, 850−859.

(32) Ara, I.; Falvello, L. R.; Forniés, J.; Lalinde, E.; Martín, A.; Martínez, F.; Moreno, M. T. *Organometallics* **1997**, *16*, 5392−5405.

(33) Kaesz, H. D.; Saillant, R. B. *Chem. Rev.* **1972**, *72*, 231−281.

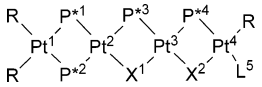

Figure 1. Atom-numbering scheme for NMR discussion purposes.

The signal due to H^1 (see Figure 1 for atom numbering) appears at −4.0 ppm as a broad triplet (57 Hz), indicating the same coupling value between H^1 and the two P atoms in trans positions, P^1 and P.[4] The signal due to H^2 is a doublet [$^2J(P^3,H^2) = 54$ Hz] centered at −6.6 ppm. Both signals are flanked by platinum satellites from which $^1J(Pt^2,H^1) \approx {}^1J(Pt^3,H^1) \approx 408$ Hz and $^1J(Pt,H^2) = 450$ and 504 Hz can be measured. The $^2J(P_{trans\ to\ H},H)$ values for the hydride ligand are an indication of the bonding mode. Usually the $^2J(P_{trans\ to\ H},H)$ values for the hydride ligand are ca. 55−80 Hz for bridged hydrides, while this coupling is much larger for terminal hydrides.[9,30,31,34−36] Moreover, although there are some exceptions,[37] usually platinum hydride complexes, bridging hydrides display $^1J(Pt,H)$ values in the range 300−600 Hz, while the terminal hydrides give signals with $^1J(Pt,H)$ values in the range 800−1400 Hz.[9,30,31,34−36] All of these data are in good agreement with the proposed structure.

The ^{19}F NMR spectrum (a deuterioacetone solution) of **4** shows in the *o*-F atom region four signals with platinum satellites in a 2:2:2:2 intensity ratio. Some signals appear overlapped, and all of the values of $^3J(Pt,F)$ cannot be measured unambiguously. In the high-field region (*m*- and *p*-F atoms), four signals for the *m*-F atoms (a 2:2:2:2 intensity ratio) and four signals for the *p*-F atoms (a 1:1:1:1 intensity ratio) are observed. This pattern is in full agreement with the inequivalence of the four C_6F_5 groups in **4**. The spectrum of **5** in a deuterioacetone solution shows, in the *o*-F region, a pattern that is analogous to **4**, while in the *m*- and *p*-F atoms region, the signals appear overlapped (see the Experimental Section).

The ^{31}P NMR spectra of **4** and **5** in a deuterioacetone solution show four signals, and the different values of the chemical shifts of the four inequivalent P atoms are conclusive in establishing their structural disposition. All data are given in Table 1. The signals due to P^1 and P^2 (see Figure 1 for atom numbering) appear at high field (from −126.8 to −142.0 ppm), as is expected for P atoms of the PPh_2 groups in the "$(C_6F_5)_2Pt(\mu\text{-}PPh_2)_2Pt$" fragment without a metal−metal bond.[13,26,38−40] For complex **4**, the signals due to P^3 and P^4 atoms appear at −32.0 and −47.9 ppm, respectively, in the range observed for all of our derivatives that display the bridged system "$M(\mu\text{-}PPh_2)(\mu\text{-}X)M$" (X = Cl, Br, I, OH) without a metal−metal bond.[1,5,39] Nevertheless, the signals due to P^3 and P^4 atoms in **5** are observed at lower field, 96.0 and 95.4 ppm, respectively. These values are in the range found in our complexes with short Pt−Pt distances in the "$Pt(\mu\text{-}PPh_2)Pt$" and "$Pt(\mu\text{-}PPh_2)(\mu\text{-}H)Pt$" fragments.[15,18,31,41] The P^1 and P^2 signals are broad, as we have usually found in all of our complexes with the "$(C_6F_5)_2Pt(\mu\text{-}PPh_2)_2Pt$" fragment, probably because of the poorly resolved couplings with the F atoms of the C_6F_5 groups.[19] In both complexes, the P^2 signal appears as a doublet of doublets (306 and 167 Hz, **4**; 249 and 122 Hz, **5**) due to the coupling with P^3 and P^1 (see Table l) and the P^3 signal as a doublet. It is noteworthy that the splitting of the P^1 and P^4 signals is different for **4** and **5**. In complex **4**, P^1 appears as a doublet (coupled with P^2, 167 Hz) and P^4 is a singlet. In complex **5**, P^1 appears as a doublet of doublets (122 and ca. 43 Hz) and P^4 as a doublet (43 Hz). The coupling between P^1 and P^4 observed in the hydrido derivative **5** (60 valence electron count) but not in the bromo derivative **4** (64 valence electron count) is in agreement[12,18] with the existence or not of a metal−metal bond between Pt^2 and Pt^3 in **5** or **4**, respectively. All of the signals show platinum satellites from which $^1J(Pt,P)$ values can be extracted (see Table 1). The platinum satellites in the P^2 signal appear overlapped (separated by ca. 1640 Hz, **4**, and ca. 1745 Hz, **5**); thus, the two coupling values with Pt^1 or with Pt^2 have to be very similar in both complexes. The P^3 atom is bridging two Pt centers not bonded to the C_6F_5 groups, and hence the P^3 signal is sharp in both cases. It is noteworthy that in complex **5** this signal shows closed platinum satellites (143 Hz) assignable to the coupling with Pt^4, and this coupling is not observed in complex **4**, as expected. For our unsaturated complexes with short intermetallic distances, for which metal−metal bonds are proposed, we have observed that the coupling between Pt and P atoms in a Pt−M−P system ["$Pt(\mu\text{-}PPh_2)_2M-P$",[15,18,26] "$Pt(\mu\text{-}PPh_2)M-P$",[12,18,31] and "$Pt(\mu\text{-}PPh_2)(\mu\text{-}H)Pt-P$"[31,42] fragments) can be measured, while this Pt−P coupling cannot be observed for saturated complexes with longer Pt···M distances. The values of these $^2J(Pt,P)$ couplings are in agreement with the assignment of the 143-Hz splitting in **5** to $^2J(Pt^4,P^3)$. Although attempts to obtain a crystal of **5** suitable for X-ray study have been unsuccessful, the 60 valence electron count for a tetranuclear complex along with the ^{31}P NMR data [$\delta(P^3)$, $\delta(P^4)$, $^3J(P^1,P^4)$, and $^2J(Pt^4,P^3)$] and the comparison with the trinuclear [$\{(C_6F_5)(PPh_3)Pt(\mu\text{-}PPh_2)(\mu\text{-}H)\}_2Pt$][31,42] are in agreement with those of the proposed structure with two Pt−Pt bonds in **5**. All of these observations point out that, because of the small size of the hydrido ligand, the Pt−Pt−Pt angles in **5** are smaller than 180°, as in [$\{(C_6F_5)(PPh_3)Pt(\mu\text{-}PPh_2)(\mu\text{-}H)\}_2Pt$], 146.84(1)°.[31]

Treatment of complex **5** with a methanol solution of HX (X = Cl, Br) in a 1:1 molar ratio yields the complexes $[NBu_4]_2[Pt_4(\mu\text{-}PPh_2)_4(\mu\text{-}H)_2(C_6F_5)_3X]$ (X = Cl, **6**; Br, **7**) as yellow solids (Scheme 1). The process that gives **6** or **7**

(34) Powell, J.; Fuchs, E.; Sawyer, J. F. *Organometallics* **1990**, *9*, 387−393.
(35) Venanzi, L. M. *Coord. Chem. Rev.* **1982**, *43*, 251−274.
(36) Hughes, R. P.; Ward, A. J.; Golen, J. A.; Incarvito, C. D.; Rheingold, A. L.; Zakharov, L. N. *Dalton Trans.* **2004**, 2720−2727.
(37) Fortunelli, A.; Leoni, P.; Marchetti, L.; Pasquali, M.; Sbrana, F.; Selmi, M. *Inorg. Chem.* **2001**, *40*, 3055−3060.
(38) Forniés, J.; Fortuño, C.; Navarro, R.; Martínez, F.; Welch, A. J. *J. Organomet. Chem.* **1990**, *394*, 643−658.
(39) Alonso, E.; Forniés, J.; Fortuño, C.; Tomás, M. *J. Chem. Soc., Dalton Trans.* **1995**, 3777−3784.
(40) Alonso, E.; Casas, J. M.; Forniés, J.; Fortuño, C.; Martín, A.; Orpen, A. G.; Tsipis, C. A.; Tsipis, A. C. *Organometallics* **2001**, *20*, 5571−5582.
(41) Alonso, E.; Forniés, J.; Fortuño, C.; Martín, A.; Orpen, A. G. *Chem. Commun.* **1996**, 231−232.
(42) Ara, I.; Chaouche, N.; Forniés, J.; Fortuño, C.; Kribii, A.; Tsipis, A. C.; Tsipis, C. A. *Inorg. Chim. Acta* **2005**, *358*, 1377−1385.

Table 1. ^{1}H and $^{31}P\{^{1}H\}$ NMR Data for Complexes **4**−**8** (*J*/Hz)

	4	**5**	**6**	**7**	**8**[a]
$\delta(H^1)$		−4.0 (t)	−4.4 (t)	−4.3(t)	−3.7(t)
$\delta(H^2)$		−6.6 (d)	−6.1 (d)	−6.2(d)	−5.9(d)
$J(P^{1\text{ or }4},H^1)$		57	63	60	61
$J(P^3,H^2)$		54	42	45	40
$J(Pt^{2\text{ or }3},H^1)$		408	520	*b*	530
$J(Pt^{3\text{ or }4},H^2)$		450	388	*b*	480
		504	582	*b*	480
$\delta(P^1)$	−131.7 (d)	−126.8 (dd)	−114.2 (dd)	−115.5(br d)	−123.1(dd)
$\delta(P^2)$	−142.0(dd)	−136.6 (dd)	−124.1 (dd)	−125.6(dd)	−135.6(dd)
$\delta(P^3)$	−32.0(d)	96.0 (d)	93.8 (d)	93.7(d)	96.6(d)
$\delta(P^4)$	−47.9 (s)	95.4 (d)	93.1 (d)	97.6(d)	104.8(dd)
$J(P^1,P^2)$	167	122	115	105	126
$J(P^1,P^4)$		43	40	41	41
$J(P^2,P^3)$	306	249	259	255	262
$J(Pt^{1\text{ or }2},P^1)$	1965	1974	1924	2000	1920
	2882	2610	2478	2500	2520
$J(Pt^{1,2},P^2)$	≈1640	≈1745	≈1800	*b*	≈1615
$J(Pt^{2\text{ or }3},P^3)$	1779	1611	1680	1675	1649
	3234	3114	2970	2950	2988
$J(Pt^{3\text{ or }4},P^4)$	2116	2021	3170	3162	1869
	3248	3044	3170	3162	3139
$J(Pt^4,P^3)$		143	134	134	128

[a] $J(Pt^2,P^4) = 46$, $\delta(P^5Ph_3) = 20.2$, $J(P^4,P^5) = 299$, $J(Pt^4,P^5) = 2688$, $J(Pt^3,P^5) = 54$. [b] See text.

consists of the breaking of one $Pt-C_6F_5$ bond and the elimination of C_6F_5H with the formation of a Pt−X bond. This straightforward process has been largely used in our pentafluorophenyl derivatives, and it has been suggested that it takes place through an oxidative addition of HX to an anionic metal center followed by reductive elimination of C_6F_5H.[43,44] We have obtained crystals of **7** for X-ray studies. Unfortunately, the crystal decomposed before the data collection could be completed, but the incomplete set of data confirms the connectivity depicted in Scheme 1. The terminal halide ligand is expected to be easily displaced by neutral ligands. In fact, treatment of the bromo derivative **7** with $[Ag(OClO_3)PPh_3]$ results in the formation of $[NBu_4][Pt_4(\mu\text{-}PPh_2)_4(\mu\text{-}H)_2(C_6F_5)_3PPh_3]$ (**8**; Scheme 1).

The ^{1}H NMR spectra of **6**−**8** (a $CDCl_3$ solution) show signals due to the hydrogen atoms of the phenyl groups along with those due to the counterion $[NBu_4]^+$. Their relative intensities are in agreement with the proposed dianionic (**6** and **7**) or monoanionic (**8**) nature of the complexes. Moreover, the expected signals in the hydride region are observed. Their relevant data are given in Table 1. For complex **7**, the $^{1}J(Pt,H)$ values cannot be calculated unambiguously because of overlapped platinum satellites, but the patterns of the signals are like those in **5**, **6**, and **8**. The ^{19}F NMR spectra of **6** and **7** show, for the *o*-F atoms, two signals (a 4:2 intensity ratio) with platinum satellites. The pattern of the most intense signal is characteristic of two different overlapped signals. In the high-field region, two broad signals (a 4:2 intensity ratio) due to *m*-F atoms and three signals (a 1:1:1 intensity ratio) due to *p*-F atoms are observed. These spectra unambiguously indicate the inequivalence of the three C_6F_5 groups. In the spectrum of **8**, three well-separated signals are observed for the *o*-F atoms (a 2:2:2 intensity ratio), three signals (a 1:1:1 intensity ratio) are observed for the *p*-F atoms, and the signals due to the *m*-F atoms appear overlapped. The $^{31}P\{^{1}H\}$ NMR spectra of **6**−**8** show the four signals due to the four inequivalent P atoms of phosphido ligands. The values of the chemical shifts as well as the corresponding coupling constants (see Table 1) are similar to those observed for complex **5**. For complex **7**, the signal due to the P^2 atom shows overlapped platinum satellites, which unambiguously preclude calculation of the $^{1}J(Pt,^{1,2}P^2)$ values. The spectrum of complex **8** shows a doublet (299 Hz) centered at 20.2 ppm due to the P atom of the PPh_3 ligand, P^5, and the P^4 signals appears as a doublet of doublets (299 and 41 Hz), while the P^4 signal in **5**−**7** is a doublet. This value of $J(P^4,P^5) = 299$ Hz observed in complex **8** is in full agreement with the trans arrangement of both atoms, as is depicted in Scheme 1. Moreover, in complex **8**, the P^4 and P^5 signals show very closed platinum satellites because of the coupling with Pt^2 and Pt^3, respectively, $^{2}J(Pt^2,P^4) = 46$ Hz and $^{2}J(Pt^3,P^5) = 54$ Hz.

Thus, although we have not been able to carry out a full X-ray study of some of these hydrido derivatives with a 60 valence electron count, their structures have been clearly established from their NMR data. The values of $\delta(P^3)$ and $^{3}J(P^1,P^4)$ in all hydride derivatives **5**−**8** as well as the observed value of $^{2}J(Pt^2,P^4)$ in **8** are in agreement with the presence of a Pt^2-Pt^3 bond. The values of $\delta(P^4)$ and $^{2}J(Pt^4,P^3)$ in **5**−**8** as well as $^{2}J(Pt^3,P^5)$ in **8** are in agreement with the presence of a Pt^3-Pt^4 bond.

The synthesis of the asymmetric complex **4** is worthy of comment. Complex **3** was synthesized (Scheme 1) by the addition of CO to the symmetric tetranuclear $[NBu_4]_2[\{(C_6F_5)_2Pt(\mu\text{-}PPh_2)_2Pt(\mu\text{-}Cl)\}_2]$ and the elimination of the Cl^- groups, through the intermediate $[(C_6F_5)_2Pt(\mu\text{-}PPh_2)_2PtClCO]^-$. The whole process was formally the result of the substitution of two bridging chloro ligands by two terminal CO groups.

(43) Forniés, J.; Martín, A.; Martín, L. F.; Menjón, B.; Kalamarides, H. A.; Rhodes, L. F.; Day, C. S.; Day, V. W. *Chem.—Eur. J.* **2002**, *8*, 4925−4934.
(44) Usón, R.; Forniés, J.; Tomás, M.; Fandos, R. *J. Organomet. Chem.* **1984**, *263*, 253−260.

Table 2. Crystal Data and Structure Refinement for $4\cdot CH_2Cl_2$ and $9\cdot 1.4CH_2Cl_2$

	$4\cdot CH_2Cl_2$	$9\cdot 1.4CH_2Cl_2$
empirical formula	$C_{104}H_{112}F_{20}N_2Br_2P_4Pt_4\cdot CH_2Cl_2$	$C_{104}H_{112}F_{20}N_2Br_2P_4Pt_4\cdot 1.4CH_2Cl_2$
formula weight	2918.94	2952.91
T/K	150(1)	150(1)
λ/Å	0.71073	0.71073
cryst syst	triclinic	monoclinic
space group	$P\bar{1}$	$P2_1/m$
a/Å	11.1142(9)	12.334(3)
b/Å	20.549(3)	22.413(2)
c/Å	25.464(3)	19.9737(15)
α/deg	106.30(2)	90
β/deg	99.595(13)	97.706(11)
γ/deg	101.547(14)	90
V/Å^3	5313.0(10)	5471.6(14)
Z	2	2
D_c/(g cm^{-3})	1.825	1.792
$\mu_{Mo\ K\alpha}$/mm^{-1}	6.194	6.034
diffractometer	Enraf Nonius CAD4	Enraf Nonius CAD4
θ range/deg	2.0−25.0	2.0−25.0
data collected	19671	2403
independent data (R_{int})	18615 (0.0278)	10366 (0.0788)
iata/restraints/parameters	18528/8/1264	9876/30/601
GOF on F^2 [a]	1.069	1.053
final R1 ($I > 2\sigma(I)$) [b]	0.0393	0.0715
final wR2 (all data) [c]	0.0988	0.1783

[a] GOF = $[\sum w(F_o^2 - F_c^2)^2/(N_{obs} - N_{param})]^{0.5}$. [b] R1 = $\sum(|F_o| - |F_c|)/\sum|F_o|$. [c] wR2 = $[\sum w(F_o^2 - F_c^2)^2/\sum w(F_o^2)^2]^{0.5}$.

It is noteworthy that in this process the tetranuclear starting material shows one "Pt(μ-X)$_2$Pt" and two "Pt(μ-PPh$_2$)$_2$Pt" fragments while complex **3** shows one "Pt(μ-PPh$_2$)$_2$Pt" and two "Pt(μ-PPh$_2$)Pt" fragments. Complex **4** is formally the result of the reverse process: the substitution of two terminal CO ligands in **3** by two Br$^-$ groups, which act as bridging ligands. However, **4** shows one "Pt(μ-PPh$_2$)$_2$Pt" and two "Pt(μ-PPh$_2$)(μ-X)Pt" fragments, unlike the tetranuclear chloro derivative **1** (Scheme 1); i.e., the halide bridging ligands are in different structural positions in complex **1** (a very symmetric structure) and in complex **4**. Both complexes (64 valence electron count) do not require any Pt−Pt bond. To compare the two types of symmetric and asymmetric structures, we have prepared the isomer of **4**, i.e., the symmetric bromo derivative $[NBu_4]_2[\{(C_6F_5)_2Pt(\mu\text{-}PPh_2)_2Pt(\mu\text{-}Br)\}_2]$ (**9**), by a metathetical process from the well-known $[NBu_4]_2[\{(C_6F_5)_2Pt(\mu\text{-}PPh_2)_2Pt(\mu\text{-}Cl)\}_2]$.[38] All data of **9** are given in the Experimental Section, and they are analogous to those of the starting chloro derivative.[38] The study of the solid-state structure of both isomers, **4** and **9**, has been carried out by X-ray studies.

Crystal Structures of $[NBu_4]_2[\{(C_6F_5)_2Pt(\mu\text{-}PPh_2)_2Pt(\mu\text{-}Br)\}_2]\cdot 1.4CH_2Cl_2$ ($9\cdot 1.4CH_2Cl_2$) and $[NBu_4]_2[Pt_4(\mu\text{-}PPh_2)_4(\mu\text{-}Br)_2(C_6F_5)_4]\cdot CH_2Cl_2$ ($4\cdot CH_2Cl_2$). Crystal data and refinement parameters are given in Table 2. Structures of the complex ions of **9** and **4** together with the atom-labeling scheme are shown in Figures 2 and 3, respectively. Selected bond distances and angles are listed in Tables 3 and 4. The anions in both **9** and **4** are tetrametallic complexes in which the Pt atoms are bridged by diphenylphosphide and bromine ligands and the pentafluorophenyl groups are the terminal ligands. Nevertheless, while in **9** the anion is symmetric, in **4** it has a nonsymmetric arrangement. The Pt atoms lie in a crystallographic mirror plane in **9**, and this symmetry operator generates half of the molecule. The structure can be regarded as two "$(C_6F_5)_2Pt(\mu\text{-}PPh_2)_2Pt$" subunits held together by two Br atoms. The Pt atoms lie in the center of a square-planar environment. The intermetallic distances clearly indicate that there is not any metal−metal bond in the complex, in accordance with the overall electron count of 64. The Pt(2)−Pt(3) distance, 3.682(1) Å, is longer than the other two [Pt(1)−Pt(2) = 3.564(1) Å and Pt(3)−Pt(4) = 3.542(1) Å] probably because of the fact that the bridging bromine ligand is bulkier than the P atom of the diphosphido ligands, as reflected in the Pt−Br and Pt−P bond distances (see Table 3). Because of the long intermetallic separation, the Pt−P−Pt angles are quite broad [Pt(1)−P(1)−Pt(2) = 103.5(1)° and Pt(3)−P(2)−Pt(4) = 102.2(2)°] and the inner P−Pt−P ones quite narrow (around 76°; see Table 3), as

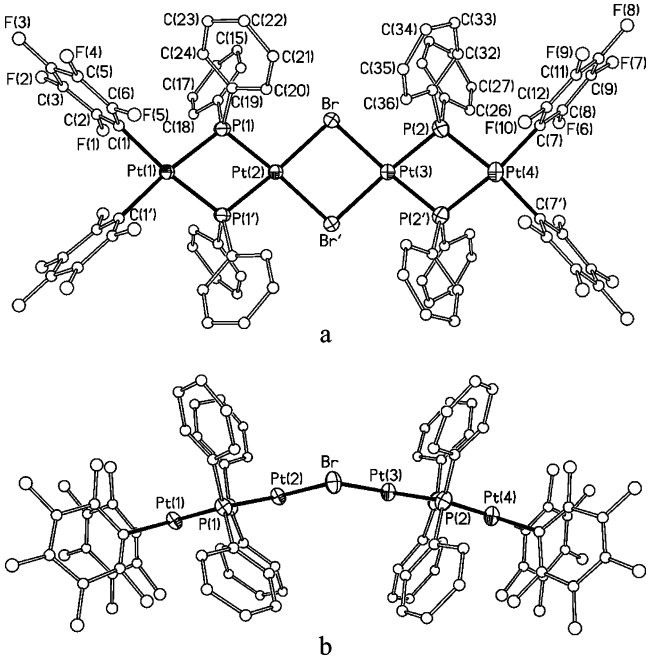

Figure 2. Two views of the molecular structure of the anion of complex $9\cdot 1.4CH_2Cl_2$.

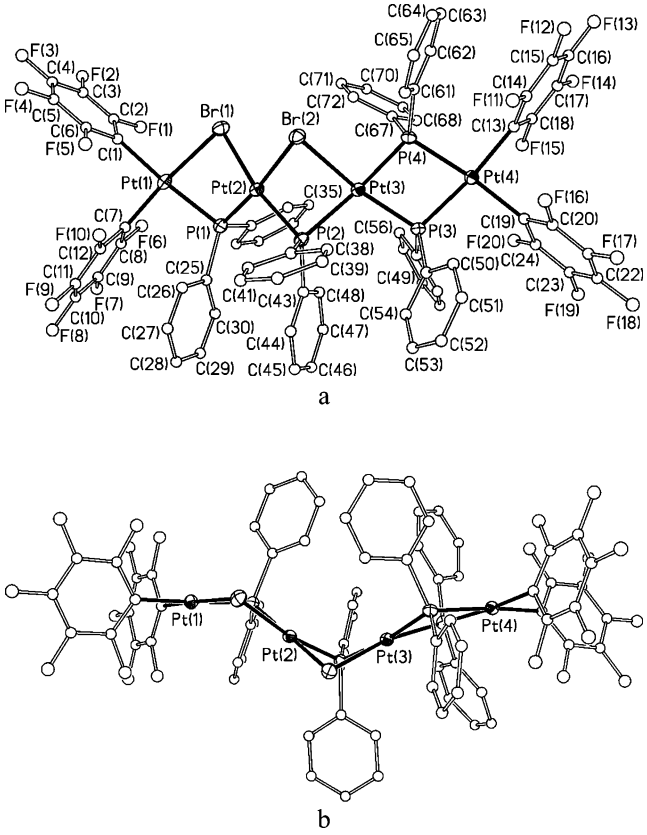

Figure 3. Two views of the molecular structure of the anion of complex **4**·CH_2Cl_2.

Table 3. Selected Bond Lengths (Å) and Angles (deg) for **9**·1.4CH_2Cl_2[a]

Pt(1)−C(1)	2.138(13)	Pt(3)−P(2)	2.255(4)
Pt(2)−Br	2.554(2)	Pt(4)−P(2)	2.296(4)
Pt(4)−C(7)	2.081(16)	Pt(2)−P(1)	2.250(4)
Pt(1)−P(1)	2.289(4)	Pt(3)−Br	2.540(2)
C(1′)−Pt(1)−C(1)	87.8(7)	C(1)−Pt(1)−P(1′)	173.8(3)
C(1)−Pt(1)−P(1)	98.2(3)	P(1′)−Pt(1)−P(1)	75.68(18)
P(1)−Pt(2)−P(1′)	77.23(19)	P(1)−Pt(2)−Br′	175.97(10)
P(1)−Pt(2)−Br	98.97(10)	Br′−Pt(2)−Br	84.79(7)
P(2)−Pt(3)−P(2′)	78.4(2)	P(2)−Pt(3)−Br	98.11(11)
P(2)−Pt(3)−Br′	176.44(11)	Br−Pt(3)−Br′	85.38(7)
C(7′)−Pt(4)−C(7)	92.2(9)	C(7)−Pt(4)−P(2)	95.5(5)
C(7)−Pt(4)−P(2′)	171.8(5)	P(2)−Pt(4)−P(2′)	76.7(2)
Pt(3)−Br−Pt(2)	92.56(5)	Pt(2)−P(1)−Pt(1)	103.49(14)
Pt(3)−P(2)−Pt(4)	102.22(16)		

[a] The symmetry transformation used to generate equivalent primed atoms is x, $0.5 - y$, z.

was previously observed in other phosphido-bridging platinum complexes.[5,13,15,18,19,31,40] Each Pt atom and the atoms bonded to it lie essentially in the same plane. The environments of the Pt atoms bridged by the diphenylphosphido ligands are almost coplanar [the dihedral angle between the best Pt(1) and Pt(2) least-squares planes is 2.8°, and that between the best Pt(3) and Pt(4) least-squares planes is 8.5°]. The whole anion is bent at the Br atoms (see Figure 2b), with the dihedral angle between the best least-squares Pt(2) and Pt(3) planes being 24.8°. The Pt−P, Pt−Br, and Pt−C distances are in the range commonly found for these kinds of complexes.[5,13,15,18,19,31,40]

In **4**, however, there are two kinds of phosphido ligands; P(3) and P(4) are simultaneously bridging the same Pt atoms

Table 4. Selected Bond Lengths (Å) and Angles (deg) for **4**·CH_2Cl_2

Pt(1)−C(7)	1.983(9)	Pt(2)−Br(1)	2.583(1)
Pt(1)−Br(1)	2.539(1)	Pt(3)−P(2)	2.325(2)
Pt(2)−Br(2)	2.546(1)	Pt(4)−C(13)	2.063(8)
Pt(3)−P(4)	2.316(2)	Pt(1)−P(1)	2.297(2)
Pt(4)−C(19)	2.060(8)	Pt(2)−P(2)	2.247(2)
Pt(4)−P(4)	2.302(2)	Pt(3)−P(3)	2.264(2)
Pt(1)−C(1)	2.075(8)	Pt(3)−Br(2)	2.606(1)
Pt(2)−P(1)	2.239(2)	Pt(4)−P(3)	2.295(2)
C(7)−Pt(1)−C(1)	90.0(3)	C(7)−Pt(1)−P(1)	94.1(2)
C(1)−Pt(1)−P(1)	175.8(3)	C(7)−Pt(1)−Br(1)	174.2(2)
C(1)−Pt(1)−Br(1)	95.6(3)	P(1)−Pt(1)−Br(1)	80.35(6)
P(1)−Pt(2)−P(2)	104.31(8)	P(1)−Pt(2)−Br(2)	172.34(6)
P(2)−Pt(2)−Br(2)	83.03(6)	P(1)−Pt(2)−Br(1)	80.48(6)
P(2)−Pt(2)−Br(1)	169.09(6)	Br(2)−Pt(2)−Br(1)	91.92(3)
P(1)−Pt(2)−Pt(3)	131.55(6)	P(2)−Pt(2)−Pt(3)	46.65(6)
Br(2)−Pt(2)−Pt(3)	52.50(2)	Br(1)−Pt(2)−Pt(3)	122.98(3)
P(3)−Pt(3)−P(4)	76.81(7)	P(3)−Pt(3)−P(2)	106.72(7)
P(4)−Pt(3)−P(2)	173.03(7)	P(3)−Pt(3)−Br(2)	167.58(6)
P(4)−Pt(3)−Br(2)	97.42(6)	P(2)−Pt(3)−Br(2)	80.25(6)
C(19)−Pt(4)−C(13)	89.0(3)	C(19)−Pt(4)−P(3)	97.4(2)
C(13)−Pt(4)−P(3)	173.3(2)	C(19)−Pt(4)−P(4)	172.7(2)
C(13)−Pt(4)−P(4)	97.2(2)	P(3)−Pt(4)−P(4)	76.47(7)
Pt(1)−Br(1)−Pt(2)	84.59(3)	Pt(2)−Br(2)−Pt(3)	76.68(3)
Pt(2)−P(1)−Pt(1)	98.93(8)	Pt(2)−P(2)−Pt(3)	88.69(7)
Pt(3)−P(3)−Pt(4)	103.02(8)	Pt(4)−P(4)−Pt(3)	101.23(8)

[Pt(3) and Pt(4)], whereas Pt(1)−Pt(2) and Pt(2)−Pt(3) are bridged by a phosphide group and a bromine group each. The intermetallic distances range from 3.197(1) to 3.569(1) Å, which again excludes any Pt−Pt bonds, as is expected for a valence electron count of 64. The replacement of the CO groups in the starting material (valence electron count of 60) with bromine ligands in **4** increases the overall number of electrons by 4. Each Pt atom lies in the center of a square-planar environment, with that of Pt(3) being the most distorted one (see Table 4). Nevertheless, as can be seen in Figure 3b, the anion complex of **4** is not planar, mainly because of the μ-Br bridging groups. The dihedral angles between the best planes around the Pt atoms are thus Pt(1)−Pt(2) = 36.9°, Pt(2)−Pt(3) = 61.6°, and Pt(3)−Pt(4) = 19.9°. The larger the value of the dihedral angle, the shorter the Pt−Pt distance: Pt(1)−Pt(2) = 3.447(1) Å, Pt(2)−Pt(3) = 3.197(1) Å, and Pt(3)−Pt(4) = 3.569(1) Å. As was previously observed in other phosphido-bridging platinum complexes, there is a relationship between the intermetallic distance and the Pt−P−Pt angle.[5,13,15,18,19,31,40] Thus, the shorter Pt(2)−Pt(3) distance is accompanied by the narrowest angle [Pt(2)−P(2)−Pt(3) = 88.7(1)°], whereas the longer Pt(3)−Pt(4) distance is observed with the broadest angles [Pt(3)−P(3)−Pt(4) = 103.0(1)° and Pt(3)−P(4)−Pt(4) = 101.2(2)°]. Like the Pt(1)−Pt(2) distance, the Pt(1)−P(1)−Pt(2) angle has an intermediate value of 98.9(1)°. Nevertheless, the Pt−P, Pt−Br, and Pt−C distances are very similar in the two isomers **9** and **4**, as can be seen in Tables 3 and 4.

To compare the reactivity of both types of isomers of $[Pt_4(\mu\text{-}PPh_2)_4(\mu\text{-}X)_2(C_6F_5)_4]^{2-}$ (X = halogen) stoichiometry (symmetric **9** and asymmetric **4**), we have studied the reactions of the asymmetric **4** with $[Ag(OClO_3)PPh_3]$ and with $AgClO_4$ (a 1:2 molar ratio). In the first case, the bromo ligands are eliminated as AgBr, and after workup of the mixture, the resulting red solid is identified (IR and NMR spectroscopy) as the dinuclear $[(C_6F_5)_2Pt(\mu\text{-}PPh_2)_2PtPPh_3]$

(**2**), with a 30 valence electron count (Scheme 1). The reaction of **4** with $AgClO_4$ renders the tetranuclear $[Pt_4(\mu\text{-}PPh_2)_4(C_6F_5)_4]$ (**10**), with a 62 valence electron count (Scheme 1). Earlier we reported that the symmetric complex **1** reacts with $[Ag(OClO_3)PPh_3]$, yielding the dinuclear **2**, and when the elimination of the Cl ligands is achieved with $AgClO_4$, the tetranuclear cluster **10** is obtained.[18,26] Moreover, the addition of PPh_3 to **10** does not yield the dinuclear derivative **2**, but rather the tetranuclear complex $[Pt_4(\mu\text{-}PPh_2)_4(C_6F_5)_4PPh_3]$ is formed.[19]

Thus, the elimination of the halo ligands as AgX from the two types of isomers yields the same derivatives. All of these results indicate that transformation between the "Pt(μ-PPh_2)$_2$Pt", "Pt(μ-PPh_2)(μ-X)Pt", and "Pt(μ-PPh_2)Pt" fragment types can be carried out easily. This fact can be understood if the possibility of the PPh_2 groups to act as a bridging ligand between three metal centers is considered.[18−20,25,41,45,46] Moreover, it is noteworthy that the nuclearity and structure of the phosphido derivatives are more dependent on the ancillary ligands than the structural arrangement of the phosphido groups in the starting materials.

Concluding Remarks

The tetranuclear derivatives described in this paper show typical square-planar metal environments with a bent arrangement of the molecular skeleton. The bending of the skeleton is strongly dependent on the bridging ligands (PPh_2 or Br).

The total valence electron count of 64 or 60 for the tetranuclear complexes implies the absence or presence of metal−metal bonds.

It is interesting to point out that the elimination of two bridging halides ($4e^-$ each) and coordination of two CO ligands is a stoichiometrically reversible process, but the starting and final resulting complexes are not the same but rather isomers; i.e., complex **1** can be transformed into **3**, but the addition of Br^- to **3** yields a complex of stoichiometry similar to that of **1** (**9**) but with a different structure.

The main structural differences in both isomers **9** and **4** seem to be related to the size of the Br^- and its position in the skeleton.

Experimental Section

General Comments. Literature methods were used to prepare the starting materials $[Pt_4(\mu\text{-}PPh_2)_4(C_6F_5)_4(CO)_2]$,[15] $[NBu_4]_2[\{(C_6F_5)_2Pt(\mu\text{-}PPh_2)_2Pt(\mu\text{-}Cl)\}_2]$,[38] and $[Ag(OClO_3)PPh_3]$.[47] C, H, and N analysis and IR and NMR spectra were performed as described elsewhere.[5] Relevant ^1H and ^{31}P NMR data are given in Table 1.

Safety Note! *Perchlorate salts of metal complexes with organic ligands are potentially explosive. Only small amounts of materials should be prepared, and these should be handled with great caution.*

Preparation of $[NBu_4]_2[Pt_4(\mu\text{-}PPh_2)_4(C_6F_5)_4(\mu\text{-}Br)_2]$ (4). To an orange solution of $[Pt_4(\mu\text{-}PPh_2)_4(C_6F_5)_4(CO)_2]$ (**3**; 0.500 g, 0.223 mmol) in CH_2Cl_2 (25 mL) was added $[NBu_4]Br$ (0.143 g, 0.446 mmol). After 12 h of stirring at room temperature, the solution was evaporated to dryness. ^{i}PrOH (5 mL) was added to the residue, and the resulting suspension was stirred for 1 h. The yellow solid was then filtered off, washed with *n*-hexane, and finally air-dried (0.449 g, 71% yield). Anal. Calcd for $C_{104}H_{112}F_{20}N_2Br_2P_4Pt_4$: C, 44.03; H, 3.95; N, 0.98. Found: C, 44.04; H, 3.76; N, 1.33. ^1H NMR (room temperature, acetone-d_6): δ from 7.8 to 6.6 (40 H, C_6H_5), 3.4 (m, 16 H, CH_2), 1.8 (m, 16 H, CH_2), 1.4 (m, 16 H, CH_2), 0.95 (t, 24 H, CH_3). ^{19}F NMR (room temperature, acetone-d_6): δ −114.9 [2 *o*-F, $^3J(^{195}Pt,F) = 262$ Hz], −115.4 [2 *o*-F, $^3J(^{195}Pt,F)$ cannot be measured], −116.3 [2 *o*-F, $^3J(^{195}Pt,F)$ cannot be measured], −116.7 [2 *o*-F, $^3J(^{195}Pt,F) = 523$ Hz], −167.5 (2 *m*-F), −167.6 (2 *m*-F), −168.0 (2 *m*-F), −168.3 (2 *m*-F), −169.0 (1 *p*-F), −169.2 (1 *p*-F), −169.5 (1 *p*-F), −169.9 (1 *p*-F).

Preparation of $[NBu_4]_2[Pt_4(\mu\text{-}PPh_2)_4(C_6F_5)_4(\mu\text{-}H)_2]$ (5). To an orange solution of **3** (0.500 g, 0.223 mmol) in CH_2Cl_2 (25 mL) was added $[NBu_4][BH_4]$ (0.172 g, 0.668 mmol). The solution was stirred at room temperature for 12 h and then evaporated to dryness. The residue was treated with $CHCl_3$ (5 mL), and after a few minutes of stirring, a yellow precipitate appears. It was filtered off, washed with *n*-hexane, and finally air-dried (0.400 g, 67% yield). Anal. Calcd for $C_{104}H_{114}F_{20}N_2P_4Pt_4$: C, 46.67; H, 4.26; N, 1.04. Found: C, 46.26; H, 4.26; N, 1.05. ^1H NMR (room temperature, acetone-d_6): δ from 7.7 to 6.6 (40 H, C_6H_5), 3.4 (m, 16 H, CH_2), 1.8 (m, 16 H, CH_2), 1.4 (m, 16 H, CH_2), 0.95 (t, 24 H, CH_3). ^{19}F NMR (room temperature, acetone-d_6): δ −112.7 [2 *o*-F, $^3J(^{195}Pt,F) = 365$ Hz], −113.1 [2 *o*-F, $^3J(^{195}Pt,F)$ cannot be measured], −113.4 [2 *o*-F, $^3J(^{195}Pt,F) = 467$ Hz], −113.6 [2 *o*-F, $^3J(^{195}Pt,F) = 349$ Hz], −166.4 (7 *m*- + *p*-F), −167.2 (1 *p*-F), −167.4 (1 *p*-F), −167.9 (3 *m*- + *p*-F).

Preparation of $[NBu_4]_2[Pt_4(\mu\text{-}PPh_2)_4(C_6F_5)_3(\mu\text{-}H)_2X]$ [X = Cl, 6; Br, 7]. To a yellow solution of **5** (0.200 g, 0.075 mmol) in CH_2Cl_2 (20 mL) kept at 0 °C was added HCl (**6**) or HBr (**7**) (0.075 mmol, MeOH/H_2O solutions). After 1 h of stirring at 0 °C, the solution was evaporated to dryness. To the residue was added ^{i}PrOH (10 mL), and the resulting solid was filtered off, washed with *n*-hexane, and finally air-dried (yield: 0.141 g, 74% (**6**); 0.171 g, 88% (**7**)).

6. Anal. Calcd for $C_{98}H_{114}F_{15}N_2ClP_4Pt_4$: C, 46.26; H, 4.52; N, 1.10. Found: C, 45.87; H, 4.90; N, 1.09. IR (cm^{-1}): ν(Pt−Cl) 271. ^1H NMR (room temperature, $CDCl_3$): δ from 8.0 to 6.6 (40 H, C_6H_5), 2.9 (m, 16 H, CH_2), 1.3 (m, 16 H, CH_2), 1.2 (m, 16 H, CH_2), 0.8 (t, 24 H, CH_3). ^{19}F NMR (room temperature, $CDCl_3$): δ −115.8 [4 *o*-F, $^3J(^{195}Pt,F) \approx 385$ Hz], −117.3 [2 *o*-F, $^3J(^{195}Pt,F) = 437$ Hz], −165.8 (1 *p*-F), −166.3 (4 *m*-F), −166.7 (2 *m*-F) −167.5 (1 *p*-F), −167.7 (1 *p*-F).

7. Anal. Calcd for $C_{98}H_{114}F_{15}N_2BrP_4Pt_4$: C, 45.46; H, 4.44; N, 1.08. Found: C, 44.98; H, 4.79; N, 1.12. ^1H NMR (room temperature, $CDCl_3$): δ from 8.0 to 6.6 (40 H, C_6H_5), 2.9 (m, 16 H, CH_2), 1.3 (m, 16 H, CH_2), 1.2 (m, 16 H, CH_2), 0.8 (t, 24 H, CH_3). ^{19}F NMR (room temperature, $CDCl_3$): δ −115.7 [4 *o*-F, $^3J(^{195}Pt,F) \approx 344$ Hz], −116.8 [2*o*-F, $^3J(^{195}Pt,F) = 433$ Hz], −165.7 (1 *p*-F), −166.3 (4 *m*-F) −166.6 (2 *m*-F), −167.3 (1 *p*-F), −167.5 (1 *p*-F).

Preparation of $[NBu_4][Pt_4(\mu\text{-}PPh_2)_4(C_6F_5)_3(\mu\text{-}H)_2PPh_3]$ (8). To a yellow solution of **7** (0.300 g, 0.116 mmol) in CH_2Cl_2 (15 mL) was added $[Ag(OClO_3)PPh_3]$ (0.054 g, 0.116 mmol). After 30 min of stirring in the darkness, the resulting suspension was filtered through Celite in order to eliminate the AgBr formed. The solution was then concentrated until approximately 1 mL and ^{i}PrOH (10 mL) was added, causing the formation of a solid, which was filtered off, washed with *n*-hexane, and finally air-dried (0.208 g, 71%

(45) Eichhofer, A.; Fenske, D.; Holstein, W. *Angew. Chem., Int. Ed. Engl.* **1993**, *32*, 242−245.
(46) Corrigan, J. F.; Doherty, S.; Taylor, N. J. *J. Am. Chem. Soc.* **1992**, *114*, 7557−7558.
(47) Cotton, F. A.; Falvello, L. R.; Usón, R.; Forniés, J.; Tomás, M.; Casas, J. M.; Ara, I. *Inorg. Chem.* **1987**, *26*, 1366−1370.

yield). Anal. Calcd for $C_{100}H_{93}F_{15}NP_5Pt_4$: C, 47.49; H, 3.71; N, 0.55. Found: C, 47.80; H, 4.17; N, 0.81. ^{1}H NMR (room temperature, $CDCl_3$): δ from 7.7 to 6.6 (55 H, C_6H_5), 3.0 (m, 8 H, CH_2), 1.5 (m, 8 H, CH_2), 1.3 (m, 8 H, CH_2), 0.9 (t, 12 H, CH_3). ^{19}F NMR (room temperature, $CDCl_3$): δ −114.9 [2 *o*-F, $^3J(^{195}$Pt,F) = 326 Hz], −115.4 [2 *o*-F, $^3J(^{195}$Pt,F) = 328 Hz], −117.3 [2 *o*-F, $^3J(^{195}$Pt,F) = 376 Hz], −165.3 (1 *p*-F), −166.4 (6 *m*-F), −167.6 (1 *p*-F), −167.7 (1 *p*-F).

Preparation of $[NBu_4]_2[\{(C_6F_5)_2Pt(\mu\text{-}PPh_2)_2Pt(\mu\text{-}Br)\}_2]$ (9). To a yellow solution of **1** (0.151 g, 0.055 mmol) in Me_2CO (20 mL) was added $AgClO_4$ (0.034 g, 0.110 mmol). After 30 min of stirring in the darkness, the resulting suspension is filtered through Celite in order to eliminate the AgCl formed. To the resulting solution was added $[NBu_4]Br$ (0.035 g, 0.110 mmol), and after 10 min of stirring, the solution was concentrated until approximately 1 mL and ^{i}PrOH (10 mL) was added, causing the formation of a solid, which was filtered off, washed with *n*-hexane, and finally dried in air (0.072 g, 46% yield). Anal. Calcd for $C_{104}H_{112}F_{20}N_2Br_2P_4Pt_4$: C, 44.03; H, 3.95; N, 0.98. Found: C, 43.97; H, 3.99; N, 1.18. IR (cm^{-1}): C_6F_5 X-sensitive mode,[48] 780, 773. ^{1}H NMR (room temperature, acetone-d_6): δ 7.7 (m, 16 *o*-H, C_6H_5), 7.1 (m, 24 *m*- + *p*-H, C_6H_5), 3.4 (m, 16 H, CH_2), 1.8 (m, 16 H, CH_2), 1.4 (m, 16 H, CH_2), 1.0 (t, 24 H, CH_3). ^{19}F NMR (room temperature, acetone-d_6): δ −110.8 [8 *o*-F, $^3J(^{195}$Pt,F) = 300 Hz], −161.2 (8 *m*-F), −161.6 (4 *p*-F). ^{31}P NMR (room temperature, acetone-d_6): δ −138.6 [$^1J(^{195}$Pt,P) = 2626 and 1926 Hz].

Reaction of 4 with $AgClO_4$. To a yellow solution of **4** (0.100 g, 0.035 mmol) in CH_2Cl_2 (20 mL) was added $AgClO_4$ (0.145 g, 0.070 mmol). After 10 min of stirring at room temperature, the resulting suspension was filtered through Celite in order to eliminate the AgBr formed. The solution was then evaporated to dryness. To the residue was added OEt_2 (25 mL), and the insoluble $[NBu_4][ClO_4]$ was filtered off. The solution was again evaporated to dryness, and the residue was treated with *n*-hexane (20 mL), filtered off, and finally air-dried. This solid was identified for its spectroscopic data[18] as **10** (0. 035 g, 46% yield).

Reaction of 4 with $[Ag(OClO_3)(PPh_3)]$. To a yellow solution of **4** (0.100 g, 0.035 mmol) in CH_2Cl_2 (20 mL) was added $[Ag(OClO_3)(PPh_3)]$ (0.033 g, 0.070 mmol), and immediately the solution turned red. After 15 min of stirring at room temperature, the resulting suspension was filtered through Celite in order to eliminate the AgBr formed. The solution was then evaporated to dryness. To the residue was added OEt_2 (25 mL), and the insoluble $[NBu_4][ClO_4]$ was filtered off. The solution was again evaporated to dryness, and the red residue was treated with *n*-hexane (20 mL), filtered off, and finally dried in air. This solid was identified for its spectroscopic data[26] as **2** (0.031 g, 32% yield).

X-ray Structure Determinations of $4\cdot CH_2Cl_2$ and $9\cdot 1.4CH_2Cl_2$. Crystal data and other details of the structure analyses are presented in Table 2. Crystals suitable for X-ray diffraction studies were obtained by slow diffusion of *n*-hexane into solutions of 0.020 g of the complexes in 3 mL of CH_2Cl_2. Absorption corrections were applied for all structures based on azimuthal scan data.

The structures were solved by Patterson and Fourier methods and refined using the program *SHELXL-97*.[49] All non-hydrogen atoms were assigned anisotropic displacement parameters. All hydrogen atoms were placed at calculated positions and constrained to ride on their parent atoms with a constrained isotropic displacement parameter. For $4\cdot CH_2Cl_2$, two methyl groups of one of the $[NBu_4]^+$ cations are disordered over two sets of positions and were refined with occupancies 0.3/0.7 [C(92)/C(92′)] and 0.5/0.5 [C(96)/C(96′)], and their distances to the methylene carbon bonded to them were constrained to idealized values. One molecule of a CH_2Cl_2 solvent is present in the structure, showing a disorder of the Cl atoms over two positions (0.65/0.35 occupancy) and sharing the same C atom. For the disordered CH_2Cl_2, the C−Cl distances were constrained to idealized geometries and all of the atoms were refined with a common anisotropic thermal parameter. For **9**, severe disorder was encountered for the C atoms of the $[NBu_4]^+$ cations, especially for the one containing the atom N(2). The possibility of a lower symmetry $P2_1$ space group was investigated but discarded on the basis of the least-squares refinement results. Because of the symmetry, the four Pt atoms, both N atoms, and two of the butyl branches of each $[NBu_4]^+$ lie in a mirror plane. C(39), which is a γ-C atom of one butyl group in the N(1) $[NBu_4]^+$ cation and should lie in this plane, is in fact disordered over two positions with partial occupancy 0.25/0.25. The C atoms of the butyl branch C(49)/C(52), belonging to the N(2) $[NBu_4]^+$ cation and which should also lie in the mirror plane, are also disordered over two positions with partial occupancy 0.25/0.25. Finally, in this same $[NBu_4]^+$ cation, C(57) and C(58) are disordered over two positions with partial occupancy 0.5/0.5. For the disordered C atoms, a common isotropic thermal parameter was used for each pair of congeners. Except for one butyl branch of the N(1) $[NBu_4]^+$ cation, the N−C and C−C distances of the cations were restrained to idealized values. Also, the C−Cl distances were restrained for the CH_2Cl_2 solvent molecule, in which the atoms were assigned a partial occupancy of 0.7. No attempts were made to include the hydrogen attached to the C atoms of the cations and solvent moieties. Full-matrix least-squares refinement on F^2 of these models converged to final residual indices given in Table 2.

Acknowledgment. We thank the Ministerio de Ciencia y Tecnología and Fondos FEDER (Project BQU2002-03997-C02-02) and DGA (Grupo Consolidado) for financial support.

Supporting Information Available: Further details of the structure determinations of $4\cdot CH_2Cl_2$ and $9\cdot 1.4CH_2Cl_2$ including atomic coordinates, bond distances and angles, and thermal parameters (CIF). This material is available free of charge via the Internet at http://pubs.acs.org.

IC051248Y

(48) Maslowsky, E., Jr. *Vibrational Spectra of Organometallic Compounds*; Wiley: New York, 1977.

(49) Sheldrick, G. M. *SHELXL-97*; University of Göttingen: Göttingen, Germany, 1997.